LAIDLAW SCHOLARS

Laidlaw Scholars Undergraduate Leadership and Research Programme

Research Report

Quantification of PTCHD1-AS Dosage at Xp22.11 in Autism Spectrum Disorder: qPCR in Human Cell Models and a CRISPRa Validation Framework

Luke Inoue

Research Advisor: Dr. Stephen Scherer

September 1, 2025

STUDENT LIFE | Centre for International Experience

UNIVERSITY OF TORONTO

Abstract

Autism spectrum disorder (ASD) frequently involves dosage-sensitive genomic loci that influence synaptic development. At Xp22.11, deletions that truncate the long non-coding RNA PTCHD1-AS are ASD risk factors. Additionally, patient iPSC-derived neurons carrying these deletions display excitatory synaptic defects consistent with NMDA-receptor hypofunction. In this Laidlaw summer project, I supported CRISPR interference (CRISPRi) experiments targeting PTCHD1-AS and quantified locus-proximal and synaptic transcripts using TaqMan qPCR. Two main observations emerged. First, across matched CRISPR-corrected (CC) and non-corrected (CNC) 1134 iPSC lines and their neuronal derivatives, ASH1L mRNA was lower in corrected material for two independent exon windows (exons 1–2 and 3–4). Second, in SK-N-BE(2) neuroblastoma cells, baseline expression for DDX53, PTCHD1-AS3 (exon 1), and PTCHD1 was stable when calibrated to TBP, providing a practical reference for future studies. These data motivate an academic-year CRISPRa overexpression study to define PTCHD1-AS dosage–response relationships and test for cis effects on PTCHD.

Acknowledgments

I thank the Laidlaw Foundation, the U of T Laidlaw Scholars Programme, and my research advisor Dr. Stephen Scherer for allowing me to research and grow my curiosity in molecular genetics. I am grateful to Dr. Carole Shum, Jill de Rijke, Natalia Rivera Alfaro and Amberlee Morgan for their day-to-day mentorship and training, as well as to the Scherer Lab and TCAG faculty for feedback and facilities.

Objectives

1. Establish laboratory baselines for PTCHD1, PTCHD1-AS3 exon 1, and DDX53 expression in SK-N-BE(2) cells using TBP as the endogenous control, to support interpretation of forthcoming studies.
2. Compare ASH1L expression across CRISPR-corrected (CC) and CRISPR-noncorrected(CNC) iPSC derived lines using exon-specific assays (exons 1-2 and 3-4), reporting calibrated fold-changes relative to the CC1134 line.

3. Define a practical CRISPRa roadmap for PTCHD1-AS overexpression in SK-N-BE(2), including target panels for synaptic and interneuron markers that are relevant to ASD biology.

Introduction

The PTCHD1/PTCHD1-AS/DDX53 region on Xp22.11 has been repeatedly implicated in neurodevelopmental risk. Early family-based studies identified PTCHD1 point mutations and microdeletions in individuals with autism spectrum disorder (ASD) and intellectual disability, highlighting this locus as dosage-sensitive and particularly relevant in males (Noor et al., 2010). Subsequent work extended the signal to PTCHD1-AS, a long non-coding RNA located adjacent to PTCHD1. Truncating deletions that reduce PTCHD1-AS expression are associated with ASD and lead to synaptic phenotypes in patient-derived iPSC neurons, including features consistent with reduced NMDA-receptor function (Ross et al., 2020). Together, these findings support a working model in which PTCHD1-AS dosage contributes to shifts in excitatory–inhibitory balance at the circuit level (Noor et al., 2010; Ross et al., 2020).

In the transcriptome and proteome phases, PTCHD1 encodes a postsynaptic protein that interacts with scaffolding partners at excitatory synapses. Loss-of-function models show cognitive and synaptic abnormalities, providing a mechanistic context for examining potential cis effects exerted by PTCHD1-AS on PTCHD1 and nearby transcripts (Ung et al., 2017; Pastore et al., 2022). Within the same genomic neighborhood, DDX53 is a single-exon RNA helicase gene embedded within the broader PTCHD1-AS locus. Recent human genetic data strengthen the case that rare DDX53 variants contribute to ASD risk, further elevating Xp22.11 as a region where noncoding regulation and local gene pathways may influence neurodevelopmental networks (Scala et al., 2025).

In addition to these locus-proximal genes, the project includes ASH1L as an epigenetic readout relevant to neuronal differentiation. ASH1L is a histone methyltransferase that deposits H3K36me2 and regulates gene programs during cortical development. Human and mouse studies link ASH1L haploinsufficiency to transcriptional dysregulation, autistic-like behaviors, and seizures, making it an informative transcript to monitor when evaluating downstream consequences of lncRNA dosage changes in developing neurons (Qin et al., 2021; Gao et al., 2021).

First, cultured SK-N-BE(2) neuroblastoma cells were given and I extracted RNA, synthesized cDNA, and performed TaqMan qPCR to validate baseline expression for PTCHD1, PTCHD1-AS3 exon 1, and DDX53, calibrated to TBP. Second, I analyzed ASH1L expression in the 1134 human iPSC line and its neuronally differentiated counterpart, comparing CRISPR-corrected (CC) and non-corrected (CNC) samples using two assays that target exon windows 1–2 and 3–4, calibrated to TFRC. Finally, I interpret these data in the context of PTCHD1-AS dosage and local gene regulation at Xp22.11 and outline how they inform a planned CRISPRa over-expression study to interrogate the gain-of-function side directly (Noor et al., 2010; Ross et al., 2020; Ung et al., 2017; Pastore et al., 2022; Scala et al., 2025; Qin et al., 2021; Gao et al., 2021).

Methods

Experimental order

All experiments were performed in the following sequence: SK-N-BE(2) cell culture, RNA extraction, cDNA synthesis, and TaqMan qPCR with relative quantification.

Cell culture: SK-N-BE(2)

SK-N-BE(2) cells were maintained in DMEM/F12. Approximately 20–30 minutes before passaging, PBS, trypsin, and growth medium were pre-warmed at 37 °C. After disinfecting the biosafety cabinet and pipettes, cultures were checked for approximately 80% confluency. A new sterile plate was prepared with 6–7 mL pre-warmed medium. Because SK-N-BE(2) has both floating and adherent cells, the spent medium was first transferred to a conical tube to retain floating cells, and the adherent monolayer was gently rinsed with 2 mL PBS. Cells were trypsinized with 1 mL trypsin for 5 minutes at 37 °C, neutralized by adding an equal volume of medium, and collected into a conical tube. The suspension was centrifuged, the supernatant was aspirated with care to avoid disturbing the pellet, and the pellet was rinsed with 1 mL PBS. Cells were resuspended in 1 mL growth medium. Counting was performed when needed for seeding densities; otherwise routine passaging at approximately 1:5 was used. Waste was decontaminated with bleach and the workspace was cleaned before closing the sash.

RNA extraction

RNA was purified using a silica spin-column workflow with on-column DNase digestion. For each sample, 350 µL homogenized lysate was mixed with 350 µL of 70% ethanol and loaded onto the column, then centrifuged for 30 seconds at ~10,150 rpm. After discarding the flow-through, 350 µL RW1 was added and centrifuged for 30 seconds. Columns received 80 µL DNase mix (10 µL DNase I + 70 µL RDD) and incubated 15 minutes at room temperature, followed by 350 µL RW1 and centrifugation. Two 500 µL RPE washes were performed (30 seconds and 2 minutes), followed by a 1-minute dry spin at approximately 12,850 rpm. RNA was eluted in 30 µL RNase-free water, and the eluate was optionally re-loaded for a second elution to maximize yield, then quantified by spectrophotometry. Bench practice included a full wipedown and RNase-Away treatment of the fume hood.

cDNA synthesis

Reverse transcription used SuperScript IV with mixed priming to capture both polyadenylated and non-polyadenylated transcripts. On ice, each annealing mix contained 0.5 µL random hexamers, 0.5 µL oligo(dT), 1 µL dNTPs, nuclease-free water, and RNA adjusted so that 2 µg total RNA occupied an 11 µL volume. Annealing proceeded 65 °C for 5 minutes, then samples were placed on ice for at least one minute. A 7 µL RT master mix per reaction included 4 µL 5× SSIV buffer, 1 µL 100 mM DTT, 1 µL RNase inhibitor, and 1 µL SuperScript IV. Reverse transcription proceeded 23 °C for 10 minutes, 55 °C for 10 minutes, and 80 °C for 10 minutes. No-template and no-RT controls accompanied each run.

TaqMan qPCR Targets and Calibration

Gene expression was quantified with Applied Biosystems TaqMan assays under standard cycling and thresholding recommendations. For the SK-N-BE(2) experiments, TBP (TATA-box binding protein; assay Hs00427620_m1) served as the endogenous control (calibrator set to 1.0).

For the 1134 CC/CNC comparisons, TFRC (transferrin receptor) served as the endogenous control for ΔCt calibration. Thermo Fisher designates TFRC as the standard copy-number reference assay in mouse (cat. 4458367) because it is reliably present in two copies and performs robustly in duplex assays; the assay maps to exon 17 (amplicon 91 bp, chr16:32,626,732, mm9) with a VIC-TAMRA probe. Although that specific product is a mouse copy-number reference assay, we used the human TFRC gene-expression assay (e.g., Hs00951083_m1) for endogenous control in human iPSC/iPSC-neuron samples, consistent with manufacturer guidance on selecting stable endogenous references for ΔΔCt analysis. Assays used to quantify targets were: ASH1L (exon 1–2 window Hs01011531_m1; exon 3–4 window Hs00218516_m1), DDX53 (Hs00704566_s1), PTCHD1 (Hs00288486_m1), and PTCHD1-AS3 exon 1 (custom assay AS3-ex1_CDDJYP2). Product pages indicate human gene targets, chromosomal positions (GRCh38), and FAM-MGB hydrolysis probe chemistry for gene-expression assays.

Table 1. Assay inventory

Target	Assay ID	Assay type	Species	Key design notes	Use in this study	Phenotype/biological context
TFRC (transferrin receptor)	Hs00951083_m1	Gene expression (FAM-MGB)	Human	GRCh38 mapping; standard GE chemistry	Endogenous control for 1134 CC/CNC ΔCt	Housekeeping/iron uptake receptor; stable expression makes it a common endogenous control.
TFRC (copy number reference)	4458367	Copy number reference (VIC-TAMRA)	Mouse	Exon 17, 91 bp, chr16:32 626,732 (mm9/NCBI37); recommended standard for mouse CNV	Cited as rationale for TFRC stability; not used directly in human expression runs	Reference assay recommended for mouse CNV studies; demonstrates TFRC stability for duplex assays.
TBP	Hs00427620_m1	Gene expression (FAM-MGB)	Human	GRCh38 mapping	Endogenous control for SK-N-BE(2)	Canonical housekeeping gene for transcription initiation.
ASH1L (exon 1-2 window)	Hs01011531_m1	Gene expression (FAM-MGB)	Human	Probe spans exons; amplicon length in 86-100 bp range	Target quantification in 1134 CC/CNC	Epigenetic writer (H3K36); dosage linked to neurodevelopment/ASD.
ASH1L (exon 3-4 window)	Hs00218516_m1	Gene expression (FAM-MGB)	Human	GRCh38 mapping; standard GE chemistry	Target quantification in 1134 CC/CNC	See box above
DDX53	Hs00704566_s1	Gene expression (FAM-MGB)	Human	GRCh38 mapping; s-design often spans exon junction	Target quantification in SK-N-BE(2)	Cancer -testis-like helicase; candidate ASD-related neighbor at Xp22.11.
PTCHD1	Hs00288486_m1	Gene expression (FAM-MGB)	Human	GRCh38 mapping	Target quantification in Sk-N-BE(2)	X-linked ASD risk gene; excitatory synaptic effects in models.
PTCHD1-AS3 exon 1	AS3-ex1_CDDJ YP2	Custom TaqMan GE	Human	Custom lncRNA assay to exon 1; designed and lab-validated	Target quantification in SK-N-BE(2)	ASD-linked lncRNA; deletions associated with NMDA hypofunction in patient neurons.

Data analysis: ΔCt/ΔΔCt workflow, QC, and error propagation

The Ct value is defined at the intersection of the amplification curve with a fixed threshold chosen within the exponential phase. Differences in Ct reflect log-scale changes because PCR products ideally double with each cycle. ΔCt was calculated as Ct(target) – Ct(reference) and ΔΔCt as ΔCt(sample) – ΔCt(calibrator). Relative quantification (RQ) was reported as 2^–ΔΔCt, with the calibrator set to RQ = 1.

Technical triplicates were required to have ΔCt standard deviation < 0.25 to be considered reliable. Curves with Ct values greater than approximately 35 cycles or with poor shape were excluded or interpreted cautiously. When amplification data were not accessible, Ct SD and ΔCt SD were used to verify replicate consistency. When biological replicates were available, group means of RQ were compared and confidence intervals reported; the range RQmin/RQmax was estimated from the standard error of ΔCt assuming a 95% confidence level.

For worked examples and spreadsheet formulas, I followed the ΔΔCt calculation pipeline that aggregates replicate Ct means, propagates standard deviations to ΔCt, preserves ΔCt variance when forming ΔΔCt (subtraction of an arbitrary constant), and converts to fold differences as 2^–ΔΔCt with an interval derived from ΔΔCt ± s. Where needed, fold changes were log2-transformed for symmetry between up- and down-regulation.

Results

ASH1L quantified with TaqMan Hs01011531_m1 (exon 1–2; TFRC-calibration)

This assay targets an exon 1–2 window in ASH1L (TaqMan Gene Expression assay Hs01011531_m1, FAM–MGB chemistry). For all 1134 cell line in this comparison, TFRC served as the endogenous control for ΔCt calibration, and CC1134 was the calibrator for ΔΔCt. Runs met the replicate and curve-quality criteria described in Methods as seen in figure 1.

In figure 2, relative to the CC1134 calibrator, the CNC1134 iPSC sample showed a 2.4-fold higher ASH1L signal. In neuronally differentiated samples from the same genetic background, 1134CNC503Nyn2 showed a 2.0-fold increase and 1134CC1003Nyn2 showed a 1.7-fold increase. The direction of effect was consistent with higher ASH1L in the non-corrected material compared with the corrected material in both iPSC and neuron contexts when measured with the exon 1–2 window.

These values are reported as 2^−ΔΔCt fold changes, calibrated to TFRC and calibrated to CC1134 set to 1.00.

ASH1L quantified with TaqMan Hs00218516_m1 (exon 3–4; TFRC-calibrated)

In figure 3, this assay targets an exon 3–4 window in ASH1L (TaqMan Gene Expression assay Hs00218516_m1, FAM–MGB chemistry). The calibration framework was the same as the exon 1–2 analysis, with TFRC as the endogenous control and CC1134 as the calibrator.

Relative to CC1134, the CNC1134 iPSC sample showed a 2.8-fold higher ASH1L signal. In neuronally differentiated counterparts, 1134CNC503Nyn2 showed a 3.5-fold increase and 1134CC1003Nyn2 showed a 1.8-fold increase. The exon 3–4 assay therefore reproduced the same overall pattern seen with exon 1–2, again indicating higher ASH1L in non-corrected material than in corrected material across both cell states.

As above, fold changes are reported as 2^−ΔΔCt values calibrated to TFRC and calibrated to CC1134 set to 1.00.

Baseline expression in SK-N-BE(2) neuroblastoma cells (TBP-calibrated)

Assays and Calibration.

Baseline measurements in SK-N-BE(2) were obtained with TaqMan Gene Expression assays targeting DDX53 (*Hs00704566_s1*), PTCHD1-AS3 exon 1 (custom, *AS3-ex1_CDDJYP2*), and PTCHD1 (*Hs00288486_m1*). TBP (*Hs00427620_m1*) served as the endogenous control. Technical triplicates were run per target. Ct thresholds were set in the exponential phase; ΔCt = Ct(target) − Ct(TBP), and relative quantity was reported as 2^−ΔCt with TBP scaled to 1.00 for ease of comparison across transcripts. No-template and no-RT controls were included for each plate.

Expression estimates.

As observed in figure 4, all three targets were detected in SK-N-BE(2) with modest variation around the endogenous control. Relative to TBP = 1.00, the mean expression values were DDX53 = 1.39, PTCHD1-AS3 exon 1 = 1.27, and PTCHD1 = 1.19. This ordering (DDX53 > PTCHD1-AS3 > PTCHD1) indicates that each gene is present at a readily quantifiable, mid-range abundance in this line, providing a practical "neutral" baseline before moving to perturbed or disease-model contexts.

Technical quality.

Replicate dispersion and curve quality met the pre-specified acceptance criteria from the Methods. Specifically, technical triplicates showed ΔCt SD < 0.25; no amplification exceeded Ct ≈ 35 cycles; and NTC/no-RT controls remained negative. TBP stability across wells supported its use as the endogenous control for this cell line. These checks suggest that the small differences among targets (approximately 1.2–1.4× relative to TBP) reflect true abundance differences rather than assay noise.

Interpretation and use as a baseline.

SK-N-BE(2) provides a clean starting point for future perturbation studies. Because all three targets sit within roughly 40% of the TBP reference, two-fold changes produced by CRISPRi/CRISPRa or by comparing to iPSC-derived neurons should be distinguishable from baseline variability using the same ΔCt/2^−ΔCt framework. The presence of detectable PTCHD1-AS3 exon 1 indicates that the custom lncRNA assay has good affinity with this line of cells, which is useful for pilot transfections and guide selection before moving to other iPSC-neuron systems.

Discussion and Conclusion

This study set out to establish a clean experimental pipeline and generate first-order evidence for how the PTCHD1/PTCHD1-AS/DDX53 region behaves in human cell models relevant to Autism Spectrum Disorder (ASD). Using a standardized workflow (cell culture → RNA extraction → cDNA synthesis → TaqMan qPCR), we (i) defined baseline expression for PTCHD1, PTCHD1-AS3 (exon 1), and DDX53 in SK-N-BE(2) cells with TBP as the reference, and (ii) compared ASH1L expression between CRISPR-corrected (CC) and non-corrected (CNC) clones from the 1134 iPSC line and matched neurons using two exon-resolved assays.

The baselines in SK-N-BE(2) were stable and well within the quantifiable range for downstream perturbations, while the CC/CNC comparison revealed a consistent directionality: CNC samples exhibited higher ASH1L than CC across both exon windows and cell states.

Interpreting the ASH1L signal

Our prior expectation—higher ASH1L in corrected material—assumed that correction removes a burden on transcription (e.g., alleviating frameshift-driven stress). The opposite pattern suggests several, not mutually exclusive, explanations:

- Compensatory regulation. CNC cells may up-regulate ASH1L to stabilize neurodevelopmental programs when other genomic perturbations are present. Because ASH1L writes H3K36 methyl marks and coordinates transcriptional elongation, even modest mRNA differences could reflect an adaptive chromatin response rather than simple loss-of-function compensation.
- Isoform and cell-state complexity. ASH1L has exon-specific regulation and produces isoforms with potentially different activities; exon 1–2 and 3–4 windows may report partially distinct transcript pools. Differentiation stage and neuronal subtype composition also modulate ASH1L output, which can decouple mRNA abundance from enzymatic activity at chromatin.
- Cis versus network effects. If PTCHD1-AS dosage perturbs local chromatin at Xp22.11, ASH1L could respond indirectly via broader transcriptional circuits rather than in a strictly local (cis) manner. The reproducibility across two exon assays argues the effect is real but does not, by itself, localize the mechanism.

Taken together, the data are most consistent with a regulatory rather than purely structural explanation—i.e., ASH1L changes reflect a shift in transcriptional programs tied to dosage biology and cell state, not just correction of a coding lesion. This aligns with prior reports that ASH1L haploinsufficiency perturbs cortical transcription and behavior in model systems, underlining ASH1L's sensitivity as an epigenetic readout in neurodevelopmental contexts (Qin et al., 2021; Gao et al., 2021).

Significance within the PTCHD1-AS dosage framework

Independent genetics and patient-cell studies point to PTCHD1-AS deletions as ASD risk factors with NMDA-receptor–linked synaptic phenotypes (Noor et al., 2010; Ross et al., 2020). Our CRISPRi summer work provides a controlled loss-of-function anchor in this framework. Establishing stable, quantitative baselines (SK-N-BE(2)) and a consistent ASH1L direction in isogenic iPSC systems creates a measurement scaffold for the next phase: directly testing whether increasing PTCHD1-AS (CRISPRa) produces reciprocal effects on PTCHD1 and DDX53 (cis influence) and shifts synaptic marker panels in directions predicted by excitatory/inhibitory (E/I) balance models. Converging evidence across CRISPRi/CRISPRa provides stronger causal inference than either perturbation alone (Gilbert et al., 2013, 2014; Chavez et al., 2015; Ross et al., 2020; Ung et al., 2018; Pastore et al., 2022).

Methodological strengths and constraints

Strengths. We used widely adopted endogenous controls (TBP; TFRC) and exon-resolved assays, ran technical replicates with clear amplification curves, and kept pre-analytical steps (cell culture, RNA extraction, cDNA synthesis) consistent to minimize batch effects. Establishing a workhorse baseline in SK-N-BE(2) reduces risk and cost when optimizing transfections and guide selection before moving into more sensitive iPSC-derived neurons.

Constraints. SK-N-BE(2) is neuroblastoma-derived and may not capture all features of developing human neurons; we therefore treat it as an engineering platform rather than a disease model.

Future Tests

During the academic year, I will develop a CRISPR activation (CRISPRa) model to test gain-of-function effects at the PTCHD1 locus. Promoter-proximal guide RNAs will be cloned into BPK1520 and co-transfected with dCas9-VPR. Initial milestones are to confirm PTCHD1-AS induction by RT-qPCR (with ddPCR if needed), establish a simple dose–response by varying guide position/number and plasmid amount, and include standard controls (non-targeting guides, empty vector, ≥3 biological replicates, a second housekeeping gene, and efficiency/standard curves to verify ΔΔCt assumptions). Optimization will be performed in SK-N-BE(2) to finalize transfection conditions and analysis, followed by replication in isogenic iPSC-derived neurons for biological relevance.

I will focus on PTCHD1 to assess potential cis effects. Results will be interpreted with the summer CRISPRi data to analyze effects across knockdown and activation. The expected outputs are a validated CRISPRa system for PTCHD1-AS, quantitative data for locus-proximal transcripts and E/I markers in two cell contexts, and a documented analysis workflow. Together, these steps should clarify PTCHD1-AS dosage–response relationships at Xp22.11 and provide a coherent foundation for subsequent functional studies if warranted.

Figures

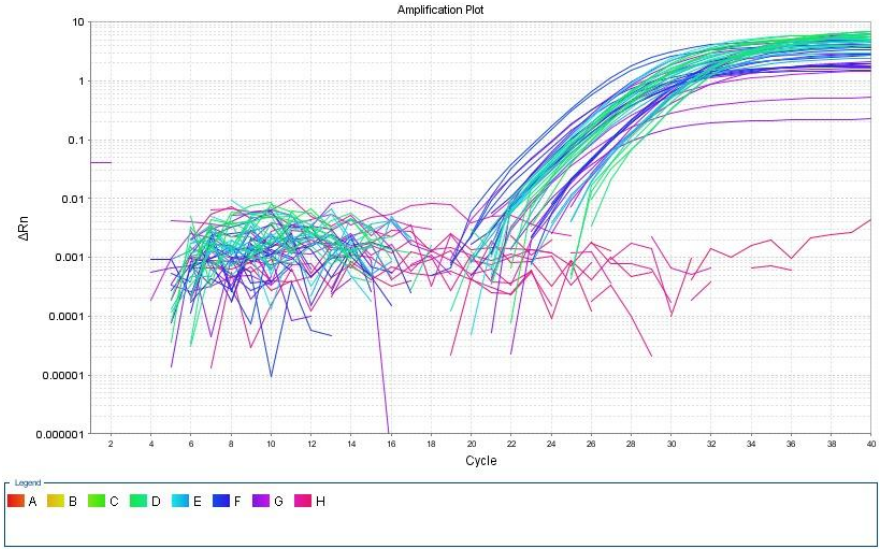

Figure 1. Amplification plot of ASH1L Exon 1-2 and 3-4, indicating the number of cycles the given sample took to double in expression.

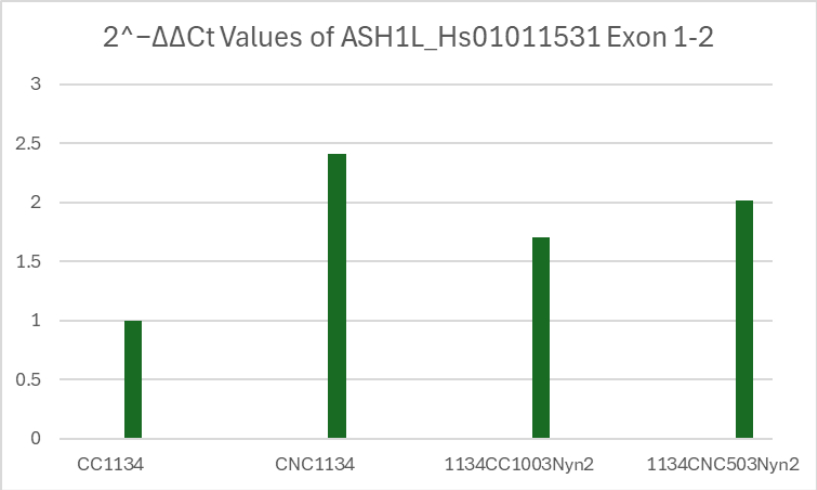

Figure 2. ASH1L Exon 1–2 fold change (calibrator CC1134): CNC1134 = 2.4×; 1134CC1003Nyn2 = 1.7×; 1134CNC503Nyn2 = 2.0×.

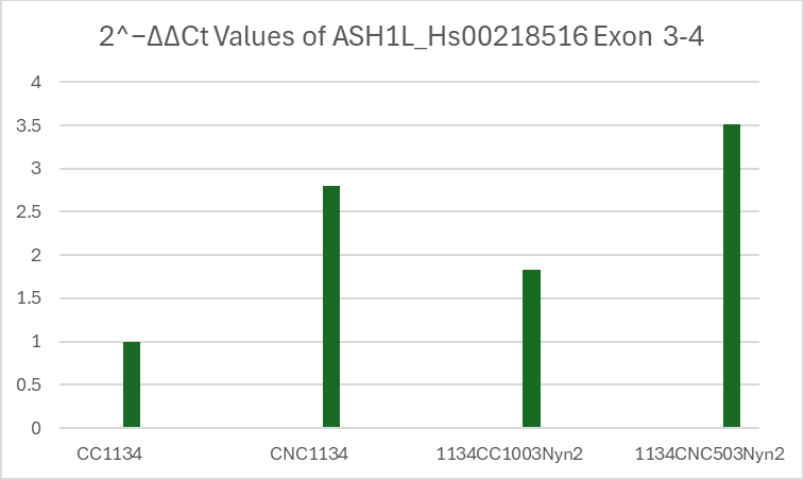

Figure 3. ASH1L Exon 3–4 fold change (calibrator CC1134): CNC1134 = 2.8×; 1134CC1003Nyn2 = 1.8×; 1134CNC503Nyn2 = 3.5×.

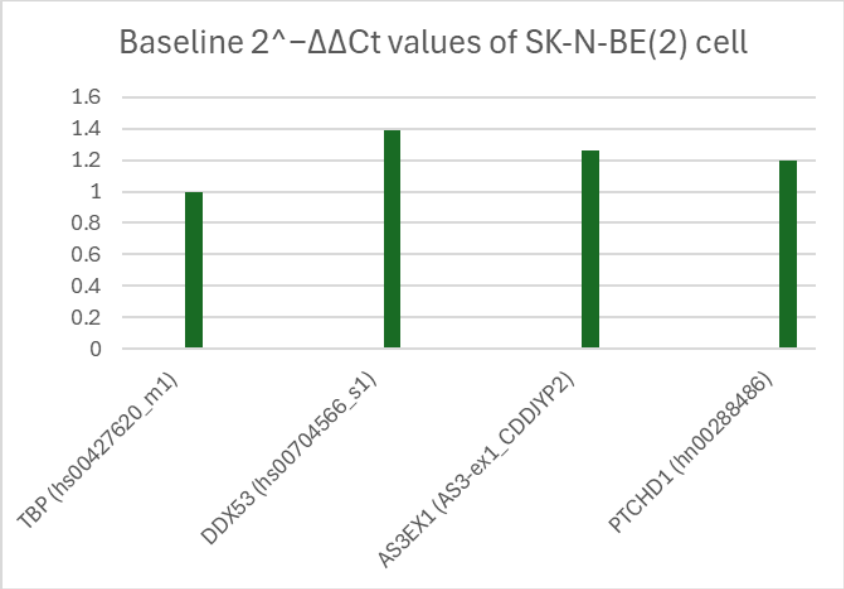

Figure 4. SK-N-BE(2) baseline calibrated to TBP = 1.0: DDX53 = 1.39; PTCHD1-AS3 (exon 1) = 1.27; PTCHD1 = 1.19.

References

.

ATCC. (n.d.). *SK-N-BE(2) (CRL-2271)*. https://www.atcc.org

Chavez, A., et al. (2015). Highly efficient Cas9-mediated transcriptional programming with VPR. *Nature Methods, 12*(4), 326–333.

Cordova, I., et al. (2024). Expansion of the genotypic and phenotypic spectrum of ASH1L-related disorders. *European Journal of Human Genetics, 32*, 847–859.

Gao, Y., et al. (2021). Loss of histone methyltransferase ASH1L in the developing mouse brain causes autistic-like behaviors. *Communications Biology, 4*, 756.

Gilbert, L. A., et al. (2013). CRISPR-mediated modular RNA-guided regulation of transcription in eukaryotes. *Cell, 154*(2), 442–451.

Gilbert, L. A., et al. (2014). Genome-scale CRISPR-mediated control of gene repression and activation. *Nature Methods, 11*(7), 703–706.

MSKCC Technology Development. (n.d.). *SK-N-BE(2): Human Neuroblastoma Cell Line*.

Noor, A., et al. (2010). Disruption at the PTCHD1 locus on Xp22.11 in autism spectrum disorder and intellectual disability. *Human Molecular Genetics, 19*(21), 4194–4206.

Pastore, S. F., et al. (2022). PTCHD1: Identification and neurodevelopmental mechanisms. *Genes, 13*(4), 694.

Ross, P. J., et al. (2020). Synaptic dysfunction in human neurons with autism-associated PTCHD1-AS deletions. *Biological Psychiatry, 87*(6), 518–529.

Scala, M., et al. (2025). Genetic variants in DDX53 contribute to autism spectrum disorder. *American Journal of Human Genetics*.

Ung, D. C., et al. (2017). Ptchd1 deficiency induces excitatory synaptic and cognitive dysfunctions. *Molecular Psychiatry, 23*(5), 1357–1373.

Procedural and analysis references (internal SOPs and teaching notes used):
SK-N-BE(2) culture SOP (lab document). Steps for warming reagents, handling floating and adherent cells, trypsinization, rinses, pelleting, and passaging ratios.

RNA extraction SOP (lab document). Spin-column protocol with ethanol binding, RW1 washes, on-column DNase digestion, RPE washes, dry spins, and elution.

cDNA synthesis SOP (lab document). SuperScript IV with mixed priming and staged temperatures.

Understanding qPCR results (University of Montreal IRIC Genomics Platform). Concepts of Ct, ΔCt, ΔΔCt, RQ, QC thresholds, and replicate criteria.

Analyzing your qRT-PCR data (teaching handout). Worked ΔΔCt examples, variance propagation, fold-change ranges, and optional log2 presentation.